Crystal Engineering

Deutsche Ausgabe: DOI: 10.1002/ange.201511444
Internationale Ausgabe: DOI: 10.1002/anie.201511444

Photoinduced Ratchet-Like Rotational Motion of Branched Molecular Crystals

*Lingyan Zhu, Rabih O. Al-Kaysi, and Christopher J. Bardeen**

Abstract: *Photomechanical molecular crystals can undergo a variety of light-induced motions, including expansion, bending, twisting, and jumping. The use of more complex crystal shapes may provide ways to turn these motions into useful work. To generate such shapes, pH-driven reprecipitation has been used to grow branched microcrystals of the anthracene derivative 4-fluoroanthracenecarboxylic acid. When these microcrystals are illuminated with light of $\lambda = 405$ nm, an intermolecular [4+4] photodimerization reaction drives twisting and bending of the individual branches. These deformations drive a rotation of the overall crystal that can be repeated over multiple exposures to light. The magnitude and direction of this rotation vary because of differences in the crystal shape, but a typical branched crystal undergoes a 50° net rotation after 25 consecutive irradiations for 1 s. The ability of these crystals to undergo ratchet-like rotation is attributed to their chiral shape.*

The use of organic photochemical reactions to power mechanical motion on nanometer to millimeter length scales is attractive due to the wide range of molecules and reactions that can be exploited.[1] The high elastic modulus and rapid response of molecular crystals make them promising candidates for photomechanical actuators.[2] Molecular crystals can undergo a variety of light-induced transformations, including expansion,[3] bending[4] and twisting,[5] curling and coiling,[6] porosity collapse,[7] and jumping.[8] If the photochemical reaction can be reversed by ambient thermal fluctuations or irradiation at a different wavelength, these motions can be repeated over many cycles.

One challenge for the field is to find ways to turn these crystal motions into useful work. Isolated crystals deform under illumination, but typically return to their original shape without a change of position. Spatially selective excitation of a single crystal can lead to translational motion,[9] and several groups have constructed devices in which crystal bending is harnessed to turn gears[10] or clamp objects,[11] but in these cases an asymmetric environment must be constructed around the crystal. Net translational motion has been observed after repeated thermal cycling of single crystals of L-pyroglutamic acid,[12] but in this case the direction of movement is random. An alternate approach is to devise a crystal shape that rotates or translates in a specific direction under repeated illuminations, analogous to a photon-powered ratchet.

Herein, we demonstrate that the key to inducing such ratchet-like motion is to make crystal shapes that are more complex than the needles and plates that have been studied so far. The photochemical reaction that drives the crystal motion is the [4+4] photodimerization that the anthracene derivative 4-fluoroanthracenecarboxylic acid (**4F-9AC**) undergoes in its crystalline form (Figure 1a). This reaction leads to the bending of crystalline microneedles and twisting of crystalline microribbons upon exposure to UV light.[13] When the light is removed, the photodimer dissociates back into monomers within about 30 s at room temperature, and the crystal reverts to its original shape. One-dimensional needles and two-dimensional ribbons are typically produced when **4F-9AC** crystals are grown on a clean water surface by slow evaporation of the solvent. For these simple shapes, repeated illumination cycles could not induce any net translation or rotation of the crystals.[13]

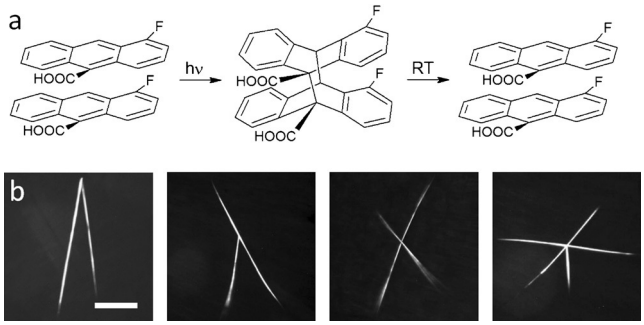

Figure 1. a) Reaction sequence of the **4F-9AC** photodimer. b) Optical microscopy images of branched crystal structures with different numbers of arms. Scale bar: 10 μm.

We decided to experiment with different growth conditions to introduce growth defects that could produce different crystal shapes. Both protonated and deprotonated forms of **4F-9AC** exist in aqueous solution, and crystal growth requires both protonation and nucleation to occur in tandem. We suspected that the combination of a chemical reaction with crystallization might lead to novel crystal shapes.[6c] When a saturated solution of **4F-9AC** in water (pH 5.5) was

[*] L. Zhu, C. J. Bardeen
Department of Chemistry, University of California, Riverside
501 Big Springs Road, Riverside, CA 92521 (USA)
E-mail: christopher.bardeen@ucr.edu
R. O. Al-Kaysi
College of Science and Health Professions-3124
King Saud bin Abdulaziz University for Health Sciences
and
King Abdullah International Medical Research Center
Ministry of National Guard Health Affairs
Riyadh 11426 (Kingdom of Saudi Arabia)

Supporting information for this article can be found under: http://dx.doi.org/10.1002/anie.201511444.

mixed with an aqueous solution containing a mineral acid, the sudden drop in the pH destabilized the equilibrium between **4F-9AC** and its conjugate base anion. The increase in protonated **4F-9AC** caused a reduction in the solubility, thereby leading to crystal growth over the course of minutes. The resulting **4F-9AC** crystals had branched shapes, as shown by the optical microscopy (Figure 1b), where the number of arms typically varied between 2 and 10. We occasionally observed highly branched "balls" with more than 20 arms.

The length of the arms could be increased by raising the growth temperature (see the Supporting Information), most likely because of temperature-enhanced Oswald ripening which favors the formation of larger crystals. Stirring the crystal suspension resulted in crystals with much shorter branches (see the Supporting Information), presumably because of breakage and introduction of multiple nucleation sites. The chemical identity of the acid had only a small effect on the growth: the acids HCl, HBr, H_3PO_4, and H_2SO_4 all yielded crystals with well-defined branches at pH 1, although the branch thickness varied slightly. Branch formation on microscope slides was robust with respect to surface treatment: both hydrophobic (silanized) and hydrophilic (Piranha-treated) glass yielded branched structures, as did freshly cleaved mica. Therefore, we do not attribute branching to the influence of surface defects. A histogram of branching angles for crystals grown at 30 °C is shown in Figure 2. The angle distribution peaks strongly below 20°, thus suggesting that the two crystal growth directions are not completely independent. If the branching was due to the growth of two uncoupled crystals lying on top of each other, we would expect to see a random distribution of crossing angles. On the other hand, if the branching resulted from well-defined crystal twinning defects, we would expect the distribution to peak sharply at a single angle. The observed variability in branching angles lies between these two extremes, thus suggesting that the branching may result from kinetic growth factors, such as local pH gradients.

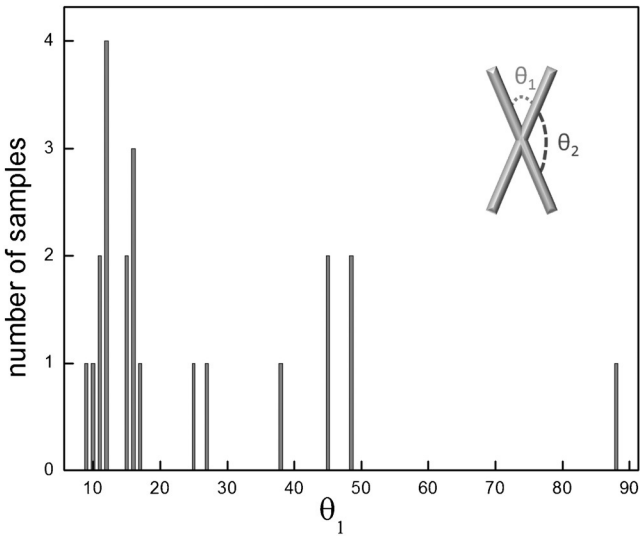

Figure 2. Histogram of branching angles for the same batch of branched crystals grown at 30 °C, with different numbers of arms. The angle θ_1 is illustrated.

The crystallinity of these branched structures was characterized by powder X-ray diffraction (PXRD) and polarized light microscopy. When the PXRD pattern of the branched crystals on a glass substrate is measured, only a single peak at $2\theta = 12°$ is observed (see the Supporting Information), which corresponds to a crystallographic plane with the (004) Miller index. If we assume that this plane is oriented parallel to the substrate, we find that the anthracene stacks run parallel to the substrate surface, similar to what was observed previously for microribbons of 9-anthracenecarboxylic acid.[5a] Polarized light microscopy confirmed that the different branches contain different crystal orientations. Figure 3a shows images of a single V-shaped crystal taken between crossed polarizers. Rotating the sample by the angle between the arms causes the different arms to become visible, thereby indicating that each arm has a single, well-defined crystal orientation within it.

The SEM images shown in Figure 3b establish that the branches actually have rectangular cross-sections, similar to other anthracene crystal microribbons studied by our group.[5a,c,14] Furthermore, the branching points are not discontinuous but evolve from a bifurcation of the parent crystal. In general, the branches are displaced from each other both vertically and horizontally. This bifurcation point may also be a weak spot in the overall crystal. Although optical microscopy showed that branched structures formed the majority (> 80 %) of the microcrystals in the growth suspension, after filtering and washing the sample on a porous anodic aluminum oxide filter for SEM imaging, the majority of the crystals were one-dimensional ribbons as a result of breakage.

The branched nature of the **4F-9AC** crystals allows them to exhibit unique photomechanical behavior. Irradiation of an individual branched crystal results in the branches undergoing a combination of twisting and bending. When the light is blocked, these distortions in the individual arms relax and the crystal returns to its original shape within 30 s. The cycle of deformation and relaxation can rotate the entire crystal about

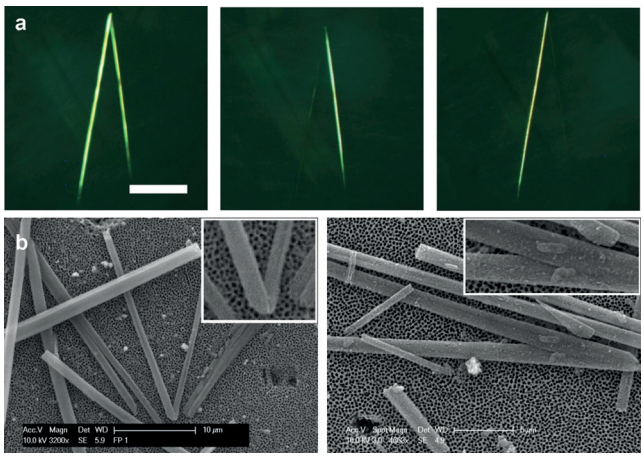

Figure 3. a) Optical microscopy images of a single V-shaped crystal taken between crossed polarizers, showing that the different arms correspond to different crystal orientations. Scale bar: 10 μm. b) SEM images of branched crystals, the inset images are the magnified branching points, showing the vertical offset.

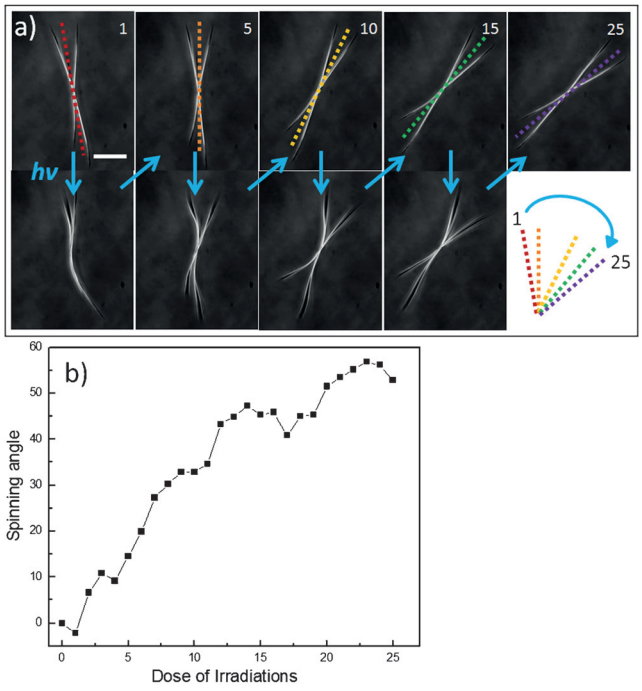

Figure 4. a) Optical microscopy images of an X-shaped crystal that rotates clockwise after each irradiation period. The cycle was repeated for 25 times. 5 cycles of the X-shaped crystal before and after irradiation are illustrated. Scale bar: 20 μm. b) Plot of the relative rotation angle as a function of radiation dose.

the bifurcation point by up to 10°. A sequence of images for an X-shaped crystal that rotates clockwise after each irradiation period is shown in Figure 4a. The light intensity at $\lambda =$ 405 nm was 0.5 W cm^{-2} and the duration of each light pulse was 1 s. The rotation angle after each dose was determined by analysis of the optical image. A plot of the relative angle as a function of radiation dose (Figure 4b) shows that although the change in angle is somewhat variable and occasionally negative, there is a consistent bias toward one direction of rotation. The net effect was to generate an overall 50° rotation after 25 consecutive irradiation doses. This behavior was generally observed, and rotation sequences and movies for other **4F-9AC** crystals are given in the Supporting Information. Sequential exposures led to a net rotation in the plane, although the magnitude and direction of this rotation varied from crystal to crystal because of their different structures (number, length, and orientation of branches). Although the rotational motion is somewhat variable, to our knowledge this is the first example of a photomechanical crystal whose shape leads to directional, ratchet-like motion after repeated exposures to irradiation.

The directional rotation suggests that the branching breaks the overall rotational symmetry of the crystal. When two different ribbons are laid on top of each other, the resulting structure is, in general, chiral. This is true for the simplest asymmetric V-shape illustrated in Figure 5 (see the Supporting Information), as well as for more complicated Y and X shapes. The combination of vertical offsets and horizontal branching is ideal for making chiral shapes. We emphasize that neither the **4F-9AC** molecule nor the crystal

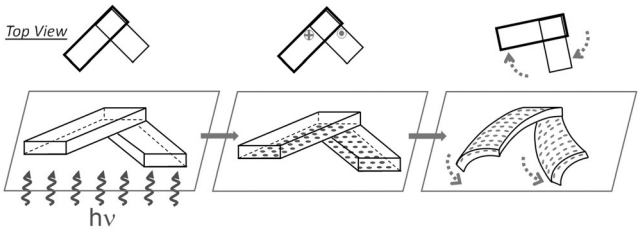

Figure 5. Mechanism for the photoinduced rotation of a chiral V-shaped microcrystal. Irradiation from the bottom creates a layer of photoproduct (ovals), whose interfacial strain drives twisting of the individual branches. The lower branch twists in a counterclockwise direction so that its edge (marked with a dot) can avoid running into the top branch. The top branch also twists counterclockwise, so its edge (marked with a +) can avoid running into the bottom branch. The net rotation of the branches sweeps the whole crystal in a clockwise direction.

packing is chiral—the chirality here is on much larger scales and is due to the shape of the crystal itself.

When a crystal has a chiral shape, release of mechanical energy can lead to rotational motion. For example, the circular motion of spiral camphor crystal shavings is powered by a combination of sublimation and dissolution.[15] For our branched crystals, the mechanical energy is supplied by the photochemistry that deforms the branches, as outlined in Figure 5. When the crystal ribbon is illuminated from below, a layer of photodimers is formed, and contraction along the molecular stacks leads to interfacial strain between the product and reactant layers.[5b] Twisting allows the two-dimensional structure to relieve the strain.[16] For an isolated ribbon, a twist in either direction should be equally effective. However, in the stacked structure in Figure 5, the twisting of the upper ribbon will encounter more resistance with a clockwise twist than with a counterclockwise twist, thus providing a bias for the twist direction. Stacking the rectangular crystal branches couples their twisting motions because the presence of the lower ribbon can affect the twist direction of the upper ribbon. Note that this structural bias is intimately connected to the chirality of the structure resulting from the vertical offset of the ribbons. The chirality leads to a bias in the twist of both ribbons, and their collective motions will occur in the same direction, at least in most cases. Although the photochemical reaction is always reversible, the strength of the surface contacts between the two branches, as well as changing interaction of the branches with the substrate, may lead to the variable motion seen in Figure 4b. Lastly, the model in Figure 5 assumes that the ribbons twist against the substrate to rotate the entire structure. In this picture, the rotation and bending requires formation of a bimorph, which depends on the direction of illumination. We found that illuminating single-branched microcrystals from the top tends to make the arms bend toward the illumination source, up and away from the substrate, and much less rotational motion is observed in this geometry. This is consistent with the bimorph mechanism, and also confirms that rotation requires the arms to interact with the surface. Thus, the rotational motion is not completely intrinsic, since it still depends on the direction of the exciting light and the presence of a surface.

We have shown that slow pH-driven reprecipitation of **4F-9AC** from an aqueous solution results in the growth of branched microcrystals. The twisting of the branches under illumination drives a rotation of the overall crystal that can be repeated over the course of many exposures to light, thereby leading to ratchet-like motion. These results demonstrate how "defective" crystal growth can result in shapes that undergo interesting and possibly useful photodriven motions.

Experimental Section

Sample preparation: **4F-9AC** was synthesized and purified according to previously described procedures.[13] To grow branched microcrystals, **4F-9AC** (1.5 mg) was added to MilliQ H_2O (25 mL), then stirred and filtered to obtain a saturated solution. 30 μL of the **4F-9AC** solution was dropped onto a microscope coverslip (22 × 40 mm) and then a drop of concentrated H_2SO_4 (30 μL, pH 0.51) was added. The branched microcrystals were obtained within 10 min. For the temperature-dependent growth, the **4F-9AC** and H_2SO_4 solutions were kept in a temperature-controlled water bath, while the cover slips were preheated on a temperature-controlled hotplate. The cover slips were kept on the same temperature-controlled hotplate during the growth of microcrystals.

X-ray diffraction measurements: **4F-9AC** branched microcrystals were grown under the same conditions and placed onto a microscope cover slip. To ensure that the majority of the branched microcrystals ended up lying flat, the sample was dried by carefully using a Kimwipe to wick away the excess water underneath the floating crystals. Powder X-ray diffraction data were collected on a PANalytical Empyrean X-ray powder diffractometer (CuK radiation, $\lambda =$ 1.5406 Å, 45 kV/40 mA power) at room temperature.

SEM measurements: The branched **4F-9AC** microcrystals were washed and filtered on an anodic aluminum oxide (AAO) membrane (Whatman, 13 mm, 20 nm) and gently washed with a solution of HCl (pH 5). The AAO membrane was dried at 40 °C in an oven for 12 h, then fixed to a piece of conducting carbon tape mounted on a SEM stub. The SEM stub was placed in a sputter coater (Cressington 108 Auto) and coated with Pt/Au for 40 s. The SEM stub was then placed inside a scanning electron microscope (XL30-FEG) for imaging.

Optical microscopy measurements: The polarized microscopy images were taken in transmission mode using a 40× 0.66 NA objective. Other images, as well as the videos of the photomechanical motion, were taken using a AMScope MU900 digital camera on an Olympus IX70 inverted microscope. The branched microcrystals were irradiated by ultraviolet light with $\lambda = 405$ nm from a filtered Hg lamp for 1 s and then allowed to recover for 1 min before the process was repeated.

Acknowledgements

This research was supported by the National Science Foundation grant DMR-1508099 (C.J.B.) and King Abdullah International Medical Research Center (KAIMRC) through grant RC10/104 (R.O.K.).

Keywords: crystal engineering · crystal growth · energy conversion · materials science

How to cite: *Angew. Chem. Int. Ed.* **2016**, *55*, 7073–7076
Angew. Chem. **2016**, *128*, 7189–7192

[1] T. Kim, L. Zhu, R. O. Al-Kaysi, C. J. Bardeen, *ChemPhysChem* **2014**, *15*, 400–414.
[2] a) N. K. Nath, M. K. Panda, S. C. Sahoo, P. Naumov, *CrystEngComm* **2014**, *16*, 1850–1858; b) J. M. Abendroth, O. S. Bushuyev, P. S. Weiss, C. J. Barrett, *ACS Nano* **2015**, *9*, 7746–7768.
[3] R. O. Al-Kaysi, A. M. Muller, C. J. Bardeen, *J. Am. Chem. Soc.* **2006**, *128*, 15938–15939.
[4] a) S. Kobatake, S. Takami, H. Muto, T. Ishikawa, M. Irie, *Nature* **2007**, *446*, 778–781; b) M. Morimoto, M. Irie, *J. Am. Chem. Soc.* **2010**, *132*, 14172–14178; c) P. Naumov, J. Kowalik, K. M. Solntsev, A. Baldridge, J.-S. Moon, C. Kranz, L. M. Tolbert, *J. Am. Chem. Soc.* **2010**, *132*, 5845–5857; d) N. K. Nath, L. Pejov, S. M. Nichols, C. Hu, N. Saleh, B. Kahr, P. Naumov, *J. Am. Chem. Soc.* **2014**, *136*, 2757–2766; e) H. Koshima, N. Ojima, H. Uchimoto, *J. Am. Chem. Soc.* **2009**, *131*, 6890–6891; f) H. Koshima, R. Matsuo, M. Matsudomi, Y. Uemura, M. Shiro, *Cryst. Growth Des.* **2013**, *13*, 4330–4337; g) O. S. Bushuyev, A. Tomberg, T. Friscic, C. J. Barrett, *J. Am. Chem. Soc.* **2013**, *135*, 12556–12559; h) O. S. Bushuyev, T. C. Corkery, C. J. Barrett, T. Friscic, *Chem. Sci.* **2014**, *5*, 3158–3164.
[5] a) L. Zhu, R. O. Al-Kaysi, C. J. Bardeen, *J. Am. Chem. Soc.* **2011**, *133*, 12569–12575; b) D. Kitagawa, H. Nishi, S. Kobatake, *Angew. Chem. Int. Ed.* **2013**, *52*, 9320–9322; *Angew. Chem.* **2013**, *125*, 9490–9492; c) T. Kim, L. Zhu, L. J. Mueller, C. J. Bardeen, *J. Am. Chem. Soc.* **2014**, *136*, 6617–6625; d) J.-K. Sun, W. Li, C. Chen, C.-X. Ren, D.-M. Pan, J. Zhang, *Angew. Chem. Int. Ed.* **2013**, *52*, 6653–6657; *Angew. Chem.* **2013**, *125*, 6785–6789.
[6] a) K. Uchida, S. Sukata, Y. Matsuzawa, M. Akazawa, J. J. D. de Jong, N. Katsonis, Y. Kojima, S. Nakamura, J. Areephong, A. Meetsma, B. L. Feringa, *Chem. Commun.* **2008**, 326–328; b) T. Kim, M. K. Al-Muhanna, S. D. Al-Suwaidan, R. O. Al-Kaysi, C. J. Bardeen, *Angew. Chem. Int. Ed.* **2013**, *52*, 6889–6893; *Angew. Chem.* **2013**, *125*, 7027–7031; c) R. O. Al-Kaysi, L. Zhu, M. Al-Haidar, M. K. Al-Muhannah, K. El-Boubbou, T. M. Hamdan, C. J. Bardeen, *CrystEngComm* **2015**, *17*, 8835–8842.
[7] M. Baroncini, S. D'Agostino, G. Bergamini, P. Ceroni, A. Comotti, P. Sozzani, I. Bassanetti, F. Grepioni, T. M. Hernandez, S. Silvi, M. Venturi, A. Credi, *Nat. Chem.* **2015**, *7*, 634–640.
[8] a) I. Colombier, S. Spagnoli, A. Corval, P. L. Baldeck, M. Giraud, A. Leaustic, P. Yu, M. Irie, *J. Chem. Phys.* **2007**, *126*, 011101; b) P. Naumov, S. C. Sahoo, B. Z. Zakharov, E. V. Boldyreva, *Angew. Chem. Int. Ed.* **2013**, *52*, 9990–9995; *Angew. Chem.* **2013**, *125*, 10174–10179; c) R. Medishetty, A. Husain, Z. Bai, T. Runceviski, R. E. Dinnebier, P. Naumov, J. J. Vittal, *Angew. Chem. Int. Ed.* **2014**, *53*, 5907–5911; *Angew. Chem.* **2014**, *126*, 6017–6021.
[9] J. T. Good, J. J. Burdett, C. J. Bardeen, *Small* **2009**, *5*, 2902–2909.
[10] F. Terao, M. Morimoto, M. Irie, *Angew. Chem. Int. Ed.* **2012**, *51*, 901–904; *Angew. Chem.* **2012**, *124*, 925–928.
[11] J. Lee, S. Oh, J. Pyo, J. M. Kim, J. H. Je, *Nanoscale* **2015**, *7*, 6457–6461.
[12] M. K. Panda, T. Runcevski, A. Husain, R. E. Dinnebier, P. Naumov, *J. Am. Chem. Soc.* **2015**, *137*, 1895–1902.
[13] L. Zhu, F. Tong, C. Salinas, M. K. Al-Muhanna, F. S. Tham, D. Kisailus, R. O. Al-Kaysi, C. J. Bardeen, *Chem. Mater.* **2014**, *26*, 6007–6015.
[14] T. Kim, L. Zhu, L. J. Mueller, C. J. Bardeen, *CrystEngComm* **2012**, *14*, 7792–7799.
[15] S. Nakata, Y. Iguchi, S. Ose, M. Kuboyama, T. Ishii, K. Yoshikawa, *Langmuir* **1997**, *13*, 4454–4458.
[16] Z. Chen, C. Majidi, D. J. Srolovitz, M. Haataja, *Appl. Phys. Lett.* **2011**, *98*, 011906.

Received: December 9, 2015
Published online: May 6, 2016

